

Supplementary figures for "Modeling oxygen transport in the brain: an efficient coarse-grid approach to capture perivascular gradients in the parenchyma".

David Pastor-Alonso<sup>1</sup>, Maxime Berg<sup>1,2</sup>, Franck Boyer<sup>3</sup>, Natalie Fomin-Thunemann<sup>4</sup>, Michel Quintard<sup>1</sup>, Yohan Davit<sup>1</sup>, Sylvie Lorthois\*<sup>1</sup>,

**1** Institut de Mécanique des Fluides de Toulouse, UMR 5502, CNRS, University of Toulouse, Toulouse, France.

**2** Department of Mechanical Engineering, University College London, London, UK

**3** Institut de Mathématiques de Toulouse (IMT), CNRS and Université de Toulouse, 31400 Toulouse, France

**4** Department of Biomedical Engineering, Boston University, Boston, Massachusetts, USA.

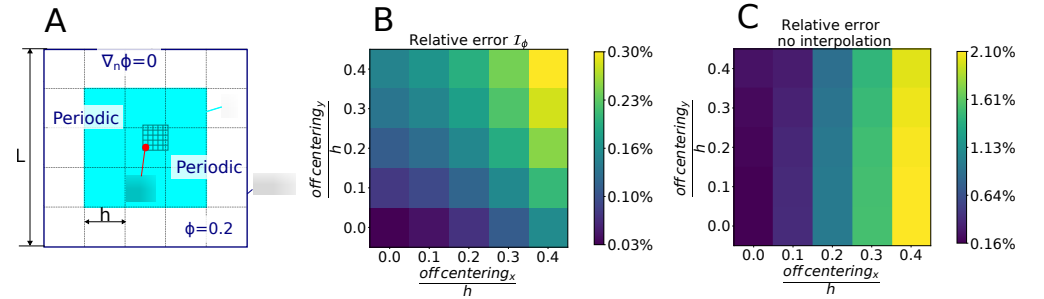


**Fig A. Flux rate errors are displayed for the off-centering of a source within a FV cell.** A: schematics of the test-case where the center of the source is moved throughout the grid contained in the upper right corner of the center cell. B and C: error on the vessel-tissue exchanges ( $\mathbf{q}$ ) with interpolation ( $\mathcal{I}_\phi$ ) in Panel B and without in Panel C. The asymmetry of errors is due to the set of boundary conditions imposed at the limits of the computational domain (see Panel A).

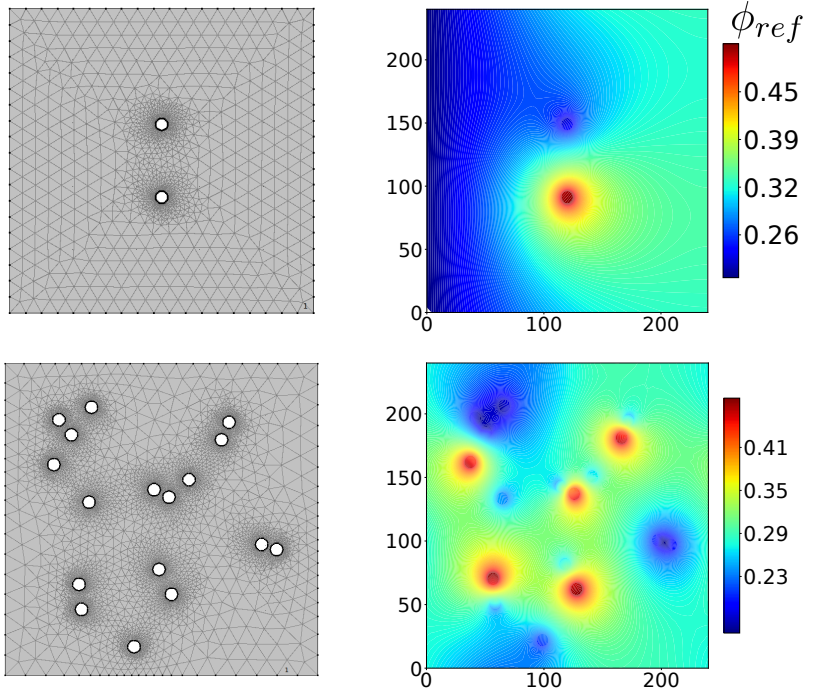


**Fig B. Fine mesh finite element (FE) reference concentration field ( $\phi_{ref}$ ) obtained with COMSOL Multiphysics for the original non-reactive BVP (eqs. 1).** For the single dipole configuration, 2278 mesh elements have been used (upper panel), while 9468 elements have been used for the multiple source configurations (lower panel).

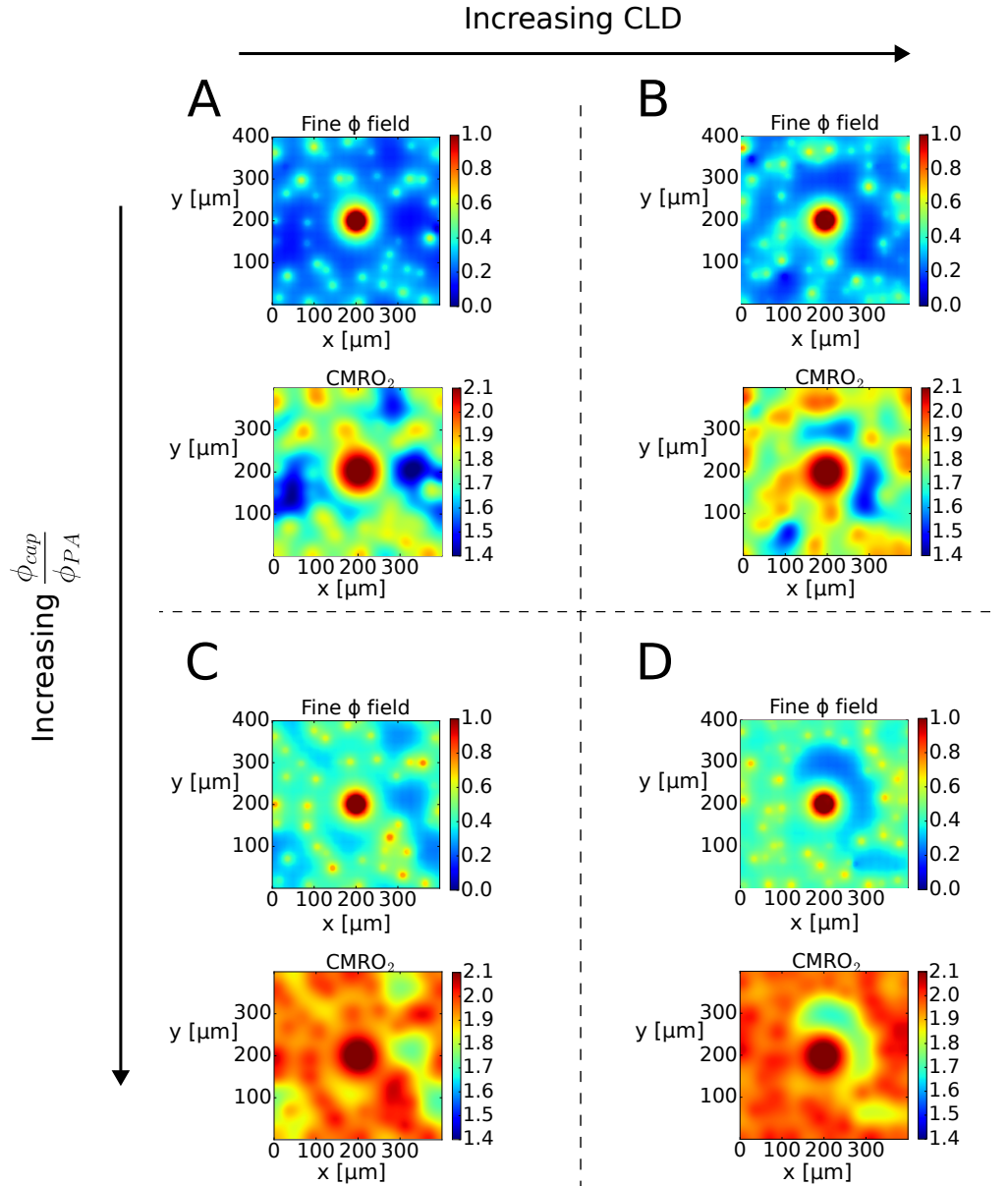


**Fig C. Sub-grid reconstructions of the concentration field (upper) and local cerebral metabolic rate  $MC/(K + C)$  (lower) for varying capillary densities and oxygenations.**  $M=2.4 \frac{\mu\text{mol}}{\text{cm}^3 \text{min}}$ . A:  $CLD=0.8 \text{ mmm}^{-3}$  and  $\phi_{cap}/\phi_{PA}=0.4$ ; B:  $CLD=1.2 \text{ mmm}^{-3}$  and  $\phi_{cap}/\phi_{PA}=0.4$ ; C:  $CLD=0.8 \text{ mmm}^{-3}$  and  $\phi_{cap}/\phi_{PA}=0.55$ ; D:  $CLD=1.2 \text{ mmm}^{-3}$  and  $\phi_{cap}/\phi_{PA}=0.55$ . To facilitate comparison, panels with same CLD present the same realization of source/sink locations.

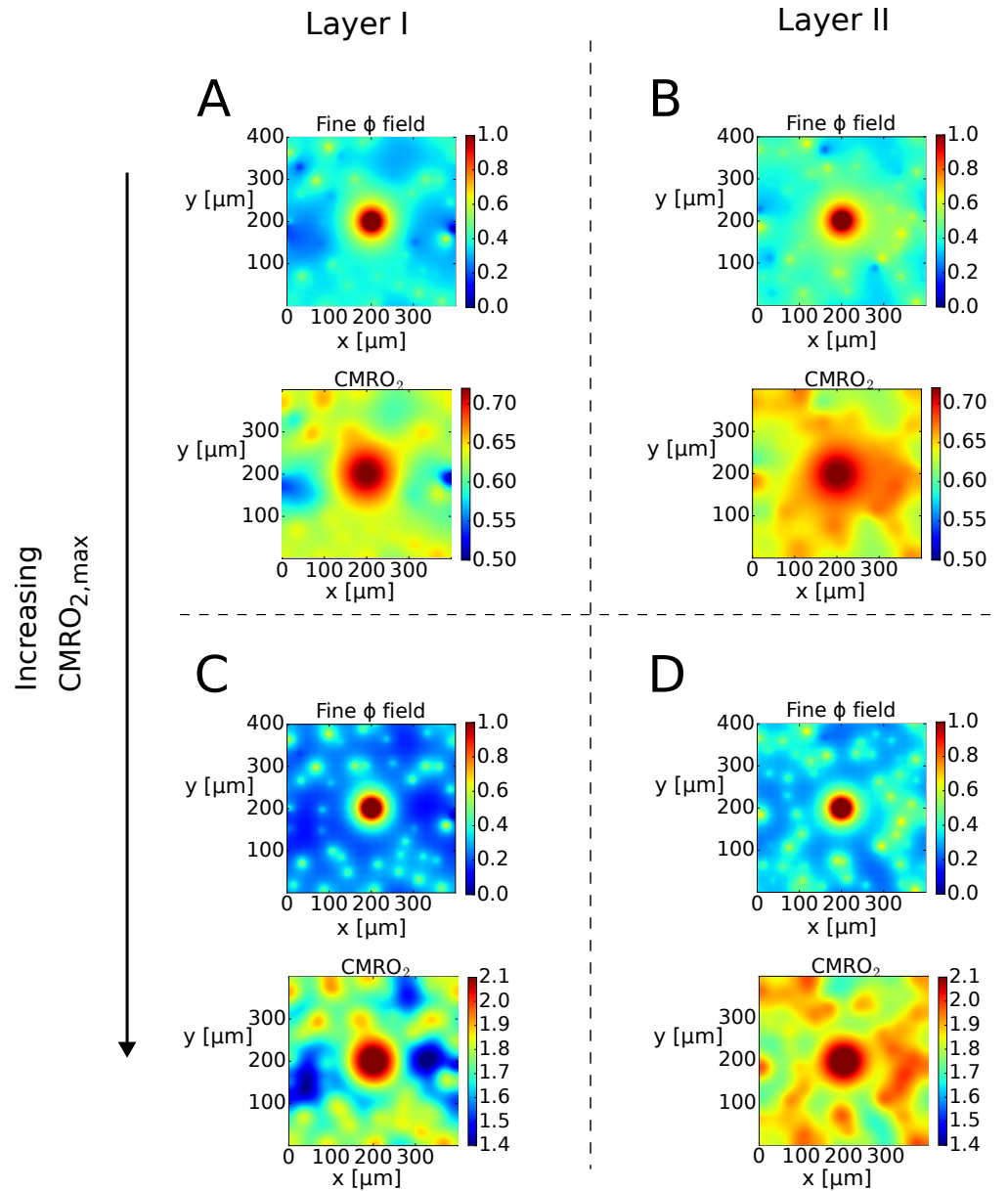


**Fig D.** Sub-grid reconstructions of the concentration field (upper) and local cerebral metabolic rate  $MC/(K + C)$  (lower) for varying values of the maximal cerebral rate of oxygen  $M$ . Layer I:  $CLD=0.8 \text{ mmm}^{-3}$  and  $\phi_{cap}/\phi_{PA}=0.4$ ; Layer II:  $CLD=0.94 \text{ mmm}^{-3}$  and  $\phi_{cap}/\phi_{PA}=0.45$ ; A and B:  $M=0.8 \frac{\mu\text{mol}}{\text{cm}^3\text{min}}$ ; C and D:  $M=2.4 \frac{\mu\text{mol}}{\text{cm}^3\text{min}}$ . To facilitate comparison, panels with same CLD present the same realization of source/sink locations.

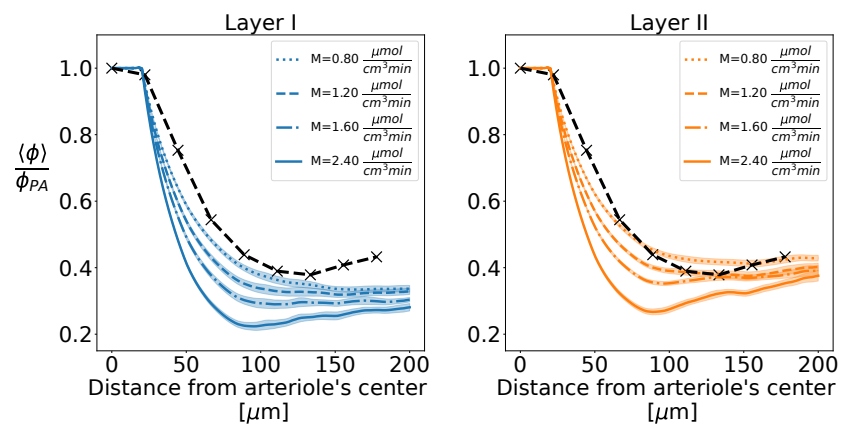


**Fig E. Radial concentration profiles predicted in layer I and layer II (thin continuous lines) together with experimental values obtained from post-processing the data in Fig. 7C (bold dashed line).** The predicted profiles are obtained by averaging the results of 30 simulations for parameters for layer I (left) and layer II (right) as given in Table 2, respectively, and for four physiologically realistic values of  $M$  (see legend in right panel). The experimental measurements were made  $100\mu\text{m}$  under the cortical surface, i.e., at the interface between layer I and II.